# Photoelectron imaging of NCCCN⁻: The triplet ground state and the singlet-triplet splitting of dicyanocarbene

Daniel J. Goebbert,[1] Kostyantyn Pichugin,[1] Dmitry Khuseynov,[1] Paul G. Wenthold,[2,a)] and Andrei Sanov[1,a)]
[1]*Department of Chemistry and Biochemistry, University of Arizona, Tucson, Arizona 84721, USA*
[2]*Department of Chemistry, Purdue University, West Lafayette, Indiana 47907, USA*

(Received 31 March 2010; accepted 5 May 2010; published online 8 June 2010)

The photoelectron spectra of $NCCCN^-$ have been measured at 355 and 266 nm by means of photoelectron imaging. The spectra show two distinct features, corresponding to the ground and first excited states of dycianocarbene. With support from theoretical calculations using the spin-flip coupled-cluster methods, the ground electronic state of HCCCN is assigned as a triplet state, while the first excited state is a closed-shell singlet. The photoelectron band corresponding to the triplet is broad and congested, indicating a large geometry change between the anion and neutral. A single sharp feature of the singlet band suggests that the geometry of the excited neutral is similar to that of the anion. In agreement with these observations, theoretical calculations show that the neutral triplet state is either linear or quasilinear ($\tilde{X}\,^3B_1$ or $^3\Sigma_g^-$), while the closed-shell singlet ($\tilde{a}\,^1A_1$) geometry is strongly bent, similar to the anion structure. The adiabatic electron binding energy of the closed-shell singlet is measured to be $3.72 \pm 0.02$ eV. The best estimate of the origin of the triplet band gives an experimental upper bound of the adiabatic electron affinity of NCCCN, $EA \leq 3.25 \pm 0.05$ eV, while the Franck–Condon modeling yields an estimate of EA(NCCCN) $= 3.20 \pm 0.05$ eV. From these results, the singlet-triplet splitting is estimated to be $\Delta E_{ST}(\tilde{X}\,^3B_1/^3\Sigma_g^- - \tilde{a}\,^1A_1) = 0.52 \pm 0.05$ eV ($12.0 \pm 1.2$ kcal/mol). © *2010 American Institute of Physics*. [doi:10.1063/1.3436717]

## I. INTRODUCTION

Carbenes have long attracted attention as intermediates in chemical reactions. It is well known that substituents $R_1$ and $R_2$ on a carbene, $R_1$-C-$R_2$, determine the electronic ground state and singlet-triplet energy splitting. The simplest carbene, $CH_2$, has a triplet ground state,[1,2] with the two same-spin nonbonding electrons occupying different, slightly nondegenerate, nonbonding *p* orbitals on the carbon atom to alleviate exchange repulsion.[3] In contrast, carbenes with $\pi$-donor substituents, particularly the halocarbenes, CHX and $CX_2$ (X=F, Cl, and Br), with the probable exception of $CI_2$, have singlet ground states.[4] In these systems, the energy splitting between the nonbonding orbitals is increased, compared to $CH_2$, as a result of $\pi$-electron donation by the halogen atoms. On the other hand, many carbenes with extended $\pi$ systems, such as diarylcarbene and acetylene carbene, have triplet ground states stabilized by $\pi$ conjugation.[5–7]

While nominally considered a "pseudohalogen," a cyanosubstituent CN does not act as a $\pi$ donor, and therefore affects carbenes more like the aryl or acetylenic groups. Indeed, cyanocarbene, HCCN, has a triplet ground state,[3,5–16] with a relatively large singlet-triplet splitting of $11.9 \pm 0.4$ kcal/mol ($0.516 \pm 0.017$ eV).[8] It is expected that adding another cyanosubstituent to give dicyanocarbene, NCCCN, should further stabilize the triplet ground state and increase the singlet-triplet splitting.

In this work, we report a combined experimental and computational studies of the structures and energetics of the electronic states of NCCCN. An *a priori* assessment of the electronic structure is shown in Fig. 1. Structure 1 (at the bottom of the figure) shows a valence-bond picture of the $NCCCN^-$ anion in the ground state. Just above it (2) are the corresponding depictions of the excited electronic state of $NCCCN^-$ at the bent and linear geometries. The linear structure is included because the excited state anion obtained by vertical excitation from the bent ground state is expected to relax toward the linearity. The neutral triplet state and two singlets are depicted in the top portion of the figure (structures 3, 4, and 5, respectively).

These representations (1–5) show the valence *p* orbitals of carbon and nitrogen atoms. For the anion ($^2B_1$ ground state), there are three electrons on the central carbon atom, with two electrons in the $a_1(\sigma)$ orbital and one electron in the $b_1(\pi)$ orbital. The anion is stabilized by incorporating more *s* orbital character into the doubly occupied orbital, which is favored in the bent geometry. Detachment of an $a_1$ electron yields the $^3B_1$ or $^1B_1$ neutral state (transitions $1 \rightarrow 3$ and $1 \rightarrow 5$ in Fig. 1, respectively), with one electron in each *p* orbital of the central carbon atom. The electronic structure of the triplet state is examined more closely in Fig. 2, which shows that the *p* electrons of the central carbon atom can participate in $\pi$ bonding with both CN groups and several linear resonance structures can be drawn. The bottom resonance structure depicted in Fig. 2 is nominally a biradical form of the carbene, where the spin density is partially sepa-

a)Electronic addresses: pgw@purdue.edu and sanov@u.arizona.edu.

 

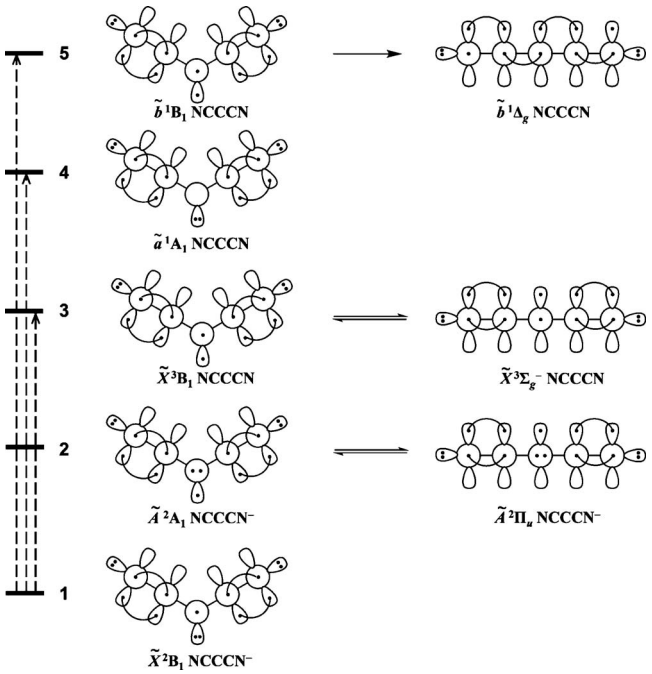


FIG. 1. Valence bond pictures of the $\pi$ bonding and low-lying electronic states of NCCCN$^-$ and NCCCN.

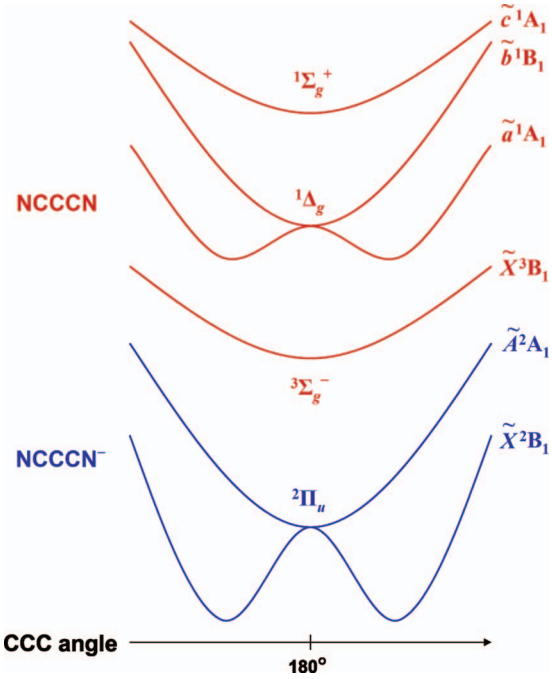


FIG. 3. Qualitative potential energy curves of NCCCN$^-$ and NCCCN as functions of the CCC bond angle based on the valence bond structures shown in Fig. 1.

rated onto both terminal nitrogens, while the top resonance structure places both unpaired electrons on one of the terminal nitrogens and is nominally a nitrene. However, it has been shown that the isoelectronic diacetylene carbene, HCCCCCH,[6,7] is best represented as two acetylenic groups connected to divalent carbon, HCC–C–CCH, with most of the unpaired electrons density localized on the central carbon. This may also be the case for NCCCN. Detachment of the $b_1$ electron from the anion (transition $1 \rightarrow 4$ in Fig. 1) gives the $^1A_1$ state of the carbene, which has a bent structure similar to the anion.

In a more general context, the electronic structure of *linear* NCCCN highlights important aspects of this molecule.

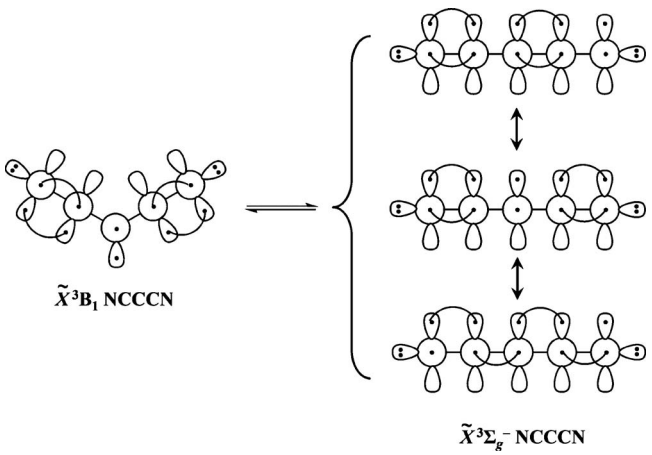


FIG. 2. Valence bond pictures of the $\pi$ bonding of $^3$NCCCN. The double arrow indicates equilibrium between the bent/linear geometries, while the three resonance structures at the linear geometry (bottom to top: biradical, carbene, and nitrene) suggest that this is the most stable geometry.

In linear NCCCN, the two nonbonding electrons occupy a pair of degenerate $\pi_u$ orbitals, resulting in three different possible electronic configurations: $^3\Sigma_g^-$, $^1\Delta_g$, and $^1\Sigma_g^+$, listed in order of increasing energy. However, NCCCN is subject to the Renner–Teller distortion (Fig. 3), which results in bent ($C_{2v}$ symmetry) molecular structures and changes the state labels to $\tilde{X}\,^3B_1$, $\tilde{a}\,^1A_1+\tilde{b}\,^1B_1$, and $\tilde{c}\,^1A_1$, respectively. In the nonlinear regime, $\tilde{X}\,^3B_1$ is the ground state, $\tilde{a}\,^1A_1$ is a closed-shell singlet, $\tilde{b}\,^1B_1$ is an open-shell singlet, and $\tilde{c}\,^1A_1$ is a higher energy closed-shell singlet, which will not be discussed further.

In a similar manner, the anion has three electrons in two nonbonding orbitals, which leads to a degenerate $^2\Pi_u$ state at the linear geometry. As with the neutral, the degeneracy is lifted by a Renner–Teller splitting, resulting in a $\tilde{X}\,^2B_1$ ground state and a $\tilde{A}\,^2A_1$ excited state. Similar to Fig. 2, the $^2A_1$ state has resonance structures with $\pi$ conjugation in the $\sigma$ plane, which may result in a linear or quasilinear structure. Qualitative potential energy curves based on the valence bond structures for NCCCN$^-$ and NCCCN with respect to the CCC bond angle are shown in Fig. 3.

The important questions that remain to be answered for NCCCN concern the structures of the singlet and triplet states and the magnitude of the singlet-triplet splitting. A previous anion photodetachment study of the cyanocarbene, HCCN$^-$, dealt with many of the same structural issues.[8] For HCCN, the triplet state is quasilinear, i.e., the bent structure is a potential minimum, while the linear form is a local maximum on the potential energy surface, but the low energy of this maximum (275 cm$^{-1}$) allows rapid interconversion of triplet HCCN. For the triplet ground state of dicyanocarbene ($^3$NCCCN, for brevity), the effect of two CN substituents

must be taken into account, but by simple analogy we might expect $^3$NCCCN to be also a linear or quasilinear molecule. Compared to HCCN, the linear NCCCN structure should be more favored due to additional $\pi$ conjugation offered by the second CN group. Moreover, the triplet state of isoelectronic HCCCCCH has been computed to be linear, suggesting that NCCCN should be linear as well.[6,7]

There have been several previous studies of NCCCN.[17–21] A matrix isolation measurement indicated a linear triplet structure,[21] but the 193 or 254 nm radiation used in that study induced isomerization between several high-energy isomers, including cyclic structures. A mass-spectrometric study with $^{13}$C labeled NCCCN$^-$ showed loss of carbon upon reionization, suggesting the carbon atoms are scrambled via these cyclic intermediates upon neutralization of the anion by high-energy collisions.[19] Theoretical studies in the same work also suggested that the triplet is linear, corresponding to the $\tilde{X}\,^3\Sigma_g^-$ state, while the lowest-energy singlet, $\tilde{a}\,^1A_1$, and the anion, $\tilde{X}\,^2B_1$, are both bent at their respective optimized geometries.[19] Coupled-cluster calculations utilizing B3LYP geometries predict the electron affinity (EA) of NCCCN($^3\Sigma_g^-$) to be 3.20 eV, while the energy splitting between the triplet and the closed-shell singlet states, $\tilde{a}\,^1A_1$, is calculated to be 0.47 eV. A more recent theoretical investigation by Kalcher[9] indicated an EA of 3.36 eV and a singlet-triplet splitting ($\tilde{X}\,^3\Sigma_g^- \rightarrow \tilde{a}\,^1A_1$) of 0.35 eV, in fair agreement with the coupled-cluster results. As with the previous work, the triplet is predicted to be linear ($\tilde{X}\,^3\Sigma_g^-$).

Another study was reported by Nguyen and co-workers,[20] who utilized complete active-space perturbation theory (CASPT2) calculations, again with B3LYP geometries, to investigate the rearrangement of NCCCN. The ground state of NCCCN was found to be linear ($^3\Sigma_g^-$) with significant spin on the terminal nitrogens, which is consistent with partial biradical character, as indicated in Fig. 2. Although the EA was not calculated in their study, the singlet-triplet splitting was determined to be 0.32 eV. However, an important result of this study was that the linear open-shell singlet, $^1\Delta_g$, was calculated to be lower in energy than the bent closed-shell singlet, $^1A_1$. Therefore, although the magnitude of the singlet-triplet splitting reported by Nguyen and co-workers[20] is similar to the values reported previously, it corresponds to a different pair of electronic states ($^3\Sigma_g^- \rightarrow {}^1\Delta_g$ in Ref. 20 versus $^3\Sigma_g^- \rightarrow {}^1A_1$ in the other works[9,19]). The $^3\Sigma_g^- \rightarrow {}^1A_1$ adiabatic excitation energy, on the other hand, was found to be 0.76 eV,[20] contrasting the 0.47 eV (Ref. 19) and 0.35 eV (Ref. 9) values reported by others.

A common theme in the studies described above is the use of geometries from density functional methods, and so it is not surprising that they all yielded linear geometries for the triplet state. This has not always been the case, however. In an early study of NCCCN using self-consistent field methods, the optimized geometry of the triplet was calculated to be bent with a central CCC angle of 132.5°, while the corresponding singlet state angle was determined to be 114.9°.[22] The interconversion barrier for the triplet state corresponding to the linear geometry was calculated to be 0.4 eV (9 kcal/mol). The calculation, however, did not include electron correlation, which is important in systems like this.[6]

The present paper reports the results of our negative-ion photoelectron imaging experiment and spin-flip (SF) coupled-cluster calculations on NCCCN$^-$ and NCCCN. The photoelectron spectrum of NCCCN$^-$ strongly resembles those that have been reported previously for other triplet ground state carbenes, such as HCH and HCCN. The photoelectron band corresponding to formation of $^3$NCCCN is broad and congested, suggesting a large geometry change upon electron detachment, as we would expect for the bent anion and linear or nearly linear $^3$NCCCN. In contrast, the singlet feature is sharp, reflecting the similar geometries of the anion and the closed-shell singlet. The open-shell singlet is not observed at the photon energy used in the experiment. Theoretical studies find $^3$NCCCN to be linear or quasilinear, depending on the level of theory and basis set used in the calculation. The computed EA and singlet-triplet splitting are consistent with the experimental results. Finally, in contrast with the previous CASPT2 results,[20] the closed-shell singlet state, $^1A_1$, is calculated to be lower in energy than the open-shell singlet state, $^1\Delta_g$.

## II. EXPERIMENTAL AND THEORETICAL METHODS

### A. The experiment and data analysis

All measurements were carried out using a negative-ion time-of-flight mass spectrometer equipped with a photoelectron imaging assembly, described in detail elsewhere.[23] Negative ions were synthesized by ion-molecule reactions in a pulsed supersonic expansion. The room-temperature vapor of malononitrile, $CH_2(CN)_2$, was seeded in $N_2O$ carrier gas at a backing pressure of ~30 psi and expanded into vacuum through a pulsed supersonic nozzle (General Valve, Series 99, Parker Hannifin, Cleveland, OH), operated at a 50 Hz repetition rate. High-energy electron collisions produced slow secondary electrons, which formed $O^-$ by dissociative electron attachment to $N_2O$. Dicyanocarbene anions were generated by the reaction of $O^-$ with malononitrile,[19,24]

$$O^- + CH_2(CN)_2 \rightarrow H_2O + C(CN)_2^-. \quad (1)$$

The ions were accelerated to 2.5 keV in a linear time-of-flight mass spectrometer. A collimated, pulsed, linearly polarized laser beam [third or forth harmonics of a Spectra Physics, Santa Clara, CA, model Lab-50 Nd:YAG (yttrium aluminum garnet) laser: 10 ns, 10 mJ at 355 nm, and 0.05 mJ at 266 nm] intersected the ions of interest within a velocity-map[25] imaging[26] assembly. Photodetached electrons were accelerated by a series of electrodes onto a 40 mm diameter dual microchannel plate detector, coupled to a P43 phosphor screen (Burle, Inc., Lancaster, PA). The resulting images were recorded by a charge-coupled device camera. Typically, $10^4$–$10^5$ experimental cycles were accumulated for each reported image.

Due to the cylindrical symmetry with respect to the laser polarization axis, images can be reconstructed using the inverse Abel transform to yield the complete three-dimensional photoelectron distributions.[27] The Abel inversion, as implemented in the BASEX program,[28] yields intensities in polar

coordinates, $I(r,\theta)$, where $r$ is the distance from the image center and $\theta$ is the angle with respect to the laboratory-frame laser polarization axis. Integration of intensities over $\theta$ yields photoelectron spectra. The energy scale was calibrated using the known photoelectron spectrum of $O^-$.[29,30] Integration over $r$ yields photoelectron angular distributions.[31,32]

### B. Theoretical methods

The low-lying electronic states of NCCCN were investigated using Krylov's SF method[33–35] combined with coupled-cluster theory. The SF approach incorporates the equation-of-motion methodology to calculate the energies of low-spin excited states, starting from the high-spin reference state and using the SF excitation operator. Unlike low-spin states, the high-spin states are not affected by orbital degeneracies and can be accurately described by a single-reference method. In the case of NCCCN, we employ the unrestricted high-spin component of the triplet state as a reference and describe the singlets and the low-spin component of the triplet as "excited" states in the space of the single spin-flipping excitations,

$$\Psi^{s,t}_{M_S=0} = \hat{R}_{M_S=-1}\Psi^{t}_{M_S=1}. \quad (2)$$

In Eq. (2), $M_S$ is the projection of the total spin and $\Psi^{t}_{M_S=1}$ is the $\alpha\alpha$ component of the triplet reference state. $\Psi^{s,t}_{M_S=0}$ represents the wave functions of the final singlet and triplet states, while $\hat{R}_{M_S=-1}$ is an excitation operator that flips the spin of one electron. A linear combination of the configurations that result from SF within one of the singly occupied orbitals creates either the $m_s=0$ triplet state, $(\alpha\beta+\beta\alpha)/\sqrt{2}$, or the open-shell singlet, $(\alpha\beta-\beta\alpha)/\sqrt{2}$. (Here, $\alpha$ and $\beta$ are the usual one electron spin functions; the latter should not be confused with the photoelectron anisotropy parameter $\beta$). An orbital change that accompanies the SF can be used to create the closed-shell singlet.

The geometries of the closed-shell singlet and the triplet states were optimized at the (U)CCSD/cc-pVTZ level of theory, whereas the open-shell singlet state was optimized by using the SF approach, SF-CCSD/cc-pVTZ. For geometry optimizations, Hartree–Fock (HF) orbitals were used as the orbital basis for the CCSD calculations. This potentially leads to a slight error due to spin contamination in the wave functions. To minimize the contamination, B3LYP orbitals were used as the orbital basis for single-point calculations. Single-point energy calculations were carried out for all states using the SF-CCSD and SF-CCSD(T) methods.[35,36] The triplet energies used in this work are those for the $M_s=0$ state, as recommended by Krylov.[37] The calculations were carried out using the QCHEM program package.[38]

## III. RESULTS

### A. Photoelectron images and spectra

The 355 and 266 nm photoelectron images of $NCCCN^-$ are shown in Fig. 4, along with the corresponding photoelectron spectra. The 266 nm spectrum in (a) shows two major overlapping features, labeled A and B. As illustrated in the figure, the overall spectrum is well fit by a sum of two overlapping Gaussian functions (relatively broad for band A and narrow for band B). Band A peaks at a binding energy of $3.53\pm0.02$ eV and has an onset around 3.2 eV (as determined by the signal rising above the noise level in the experimental spectrum). Feature B has a maximum at $3.72\pm0.02$ eV. The maximum positions are assigned as the vertical detachment energies (VDEs) of the corresponding transitions.

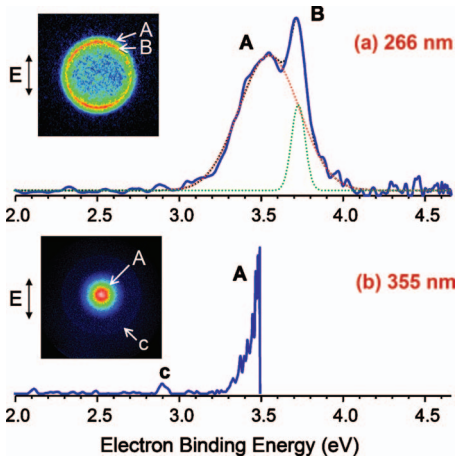


FIG. 4. Photoelectron images and spectra of $NCCCN^-$ obtained at (a) 266 nm and (b) 355 nm. The double arrows indicate the direction of laser polarization. Features A and B in the 266 nm spectrum are fit by two Gaussian functions (red and green dotted lines, respectively), which represent the Franck–Condon envelopes of the $NCCCN \leftarrow NCCCN^-$ photodetachment transitions. Band A is assigned to the $\tilde{X}\,^3B_1/^3\Sigma_g^- \leftarrow \tilde{X}\,^2B_1$ transition with VDE $=3.53\pm0.02$ eV. Band B is assigned to $\tilde{a}\,^1A_1 \leftarrow \tilde{X}\,^2B_1$, with VDE $=3.72\pm0.02$ eV. Weak feature c peaking at eBE $=2.88\pm0.02$ eV in the 355 nm spectrum is due to the photodetachment of $HC(CN)_2^-$ (Ref. 24).

The analysis of the angular distributions is complicated by the overlap of the two bands. The anisotropy parameter for band A was obtained by analyzing the 266 nm photoelectron image in the range of electron binding energy (eBE) from 3.20 to 3.60 eV, effectively excluding the energy range of band B Gaussian fitting function [see Fig. 4(a)]. Band A's anisotropy was thus determined to be $\beta=0.20\pm0.03$. The $\beta$ value for band B could not be determined because its entire spectral range includes significant overlap with feature A. The photoelectron angular distribution of the entire 266 nm image (bands A and B combined) is described by $\beta=0.19\pm0.03$.

The 355 nm photoelectron image of $NCCCN^-$ in Fig. 4(b) shows the onset of band A around eBE=3.3 eV. Similar to the 266 nm spectrum, no vibrational structure is resolved. The 355 nm spectrum shows one additional feature, a weak outer band (labeled c) with a maximum at eBE $=2.88\pm0.02$ eV and an anisotropy value of $\beta=-0.16\pm0.10$. Scanning the photodetachment laser pulse timing along the m/z=64 ($NCCCN^-$) and 65 peaks and adjusting the instrument mass resolution (which controls the degree of overlap between neighboring m/z peaks), conclusively showed that feature c belongs to the m/z=65 anion, $HC(CN)_2^-$, formed in the ion source from the same precursor used in this study. Band c position is in excellent agreement with the recently measured value of EA of dicyanomethyl radical, $2.88\pm0.01$ eV.[24] Therefore, this band will not be further discussed here.

TABLE I. Optimized geometries of $NCCCN^-$ and NCCCN electronic states [determined at the (U)CCSD/cc-pVTZ level of theory].

| | C–C bond length (Å) | C–N bond length (Å) | CCC bond angle (deg) | CCN bond angle (deg) |
|---|---|---|---|---|
| Anion ($\tilde{X}\ ^2B_1$) [a] | 1.379 | 1.173 | 119.3 | 173.7 |
| Triplet ($\tilde{X}\ ^3B_1/^3\Sigma_g^-$) [a] | 1.320 | 1.179 | 168.4 | 178.2 |
| Closed-shell singlet ($\tilde{a}\ ^1A_1$) [a] | 1.383 | 1.165 | 118.2 | 173.1 |
| Open-shell singlet ($\tilde{b}\ ^1\Delta_g$) [b] | 1.318 | 1.168 | 180 | 180 |

[a]The CCCN dihedral angle is 180°.
[b]The open-shell state was optimized by using the SF approach.

## B. Theoretical results

### 1. Molecular geometries

Theoretical calculations were carried out on the triplet, open-shell singlet, closed-shell singlet, and the radical anion states of dicyanocarbene. The optimized bond lengths and bond angles are given in Table I. The geometries of the singlet states are consistent with the previous results for this system,[9,19,22] as well as other similar carbenes (e.g., HCCN and $H_3CCCCCCH$).[7,8] The closed-shell singlet ($\tilde{a}\ ^1A_1$) structure is strongly bent (CCC bond angle 118°), similar to other simple closed-shell carbenes, including methylene.[2] Similarly, the open-shell singlet ($\tilde{b}\ ^1B_1$) optimizes to a linear geometry ($\tilde{b}\ ^1\Delta_g$), as showed previously by Nguyen and co-workers.[20]

The structure of the triplet state is more challenging to determine. At the (U)CCSD/cc-pVTZ level of theory, it is found to be slightly nonlinear, with a CCC bond angle of 168.4° (Table I). The large bond angle in the triplet state is typical for carbenes. However, the question remains whether $^3$NCCCN is truly bent. The triplet state of the isoelectronic diacetylenic carbene, HCCCCCH, has been found to be linear.[6] Similarly, whereas triplet cyanocarbene, HCCN, appears to be nonlinear, spectroscopic studies indicate that it is quasilinear, with an electronic potential barrier at linearity that is lower than the zero-point vibrational level.[8,10] We find that the optimized geometry of $^3$NCCCN is highly sensitive to the basis set and the extent of correlation included in the calculation. For example, the CCC bond angles optimized at the CCSD level of theory using the cc-pVDZ, cc-pVTZ, and cc-pVQZ basis sets are 155.6°, 168.4°, and 172.0°, respectively, indicating that the triplet state structure approaches linearity as the basis set size is increased.

In order to investigate the effect of additional correlation, we carried out single-point calculations at the SF-CCSD and SF-CCSD(T) levels with the cc-pVTZ basis set for a series of triplet state geometries optimized at the CCSD/cc-pVTZ level with the CCC bond angle fixed at selected values between 155° and 180°. The resulting energies were compared to those determined at the same level of theory with the same basis set for the fully optimized CCSD/cc-pVTZ geometry ($\angle$CCC=168.4°). The results are listed in Table II. Although the energy differences are small, lower energy structures (compared to the fully optimized CCSD/cc-pVTZ geometry) are found with different levels of theory. The difference is likely due to using B3LYP orbitals as opposed to HF orbitals for the CCSD basis in the single-point calculations.

Based on the SF-CCSD/cc-pVTZ results, the linear geometry is approximately 40 $cm^{-1}$ higher in energy than the CCSD/cc-pVTZ fully relaxed structure. The SF-CCSD(T)/cc-pVTZ calculations suggest that the linear geometry is a very shallow minimum, 6.6 $cm^{-1}$ more stable than the CCSD/cc-pVTZ fully relaxed structure with $\angle$CCC =168.4°. When diffuse functions are included in the calculation (the aug-cc-pVTZ basis set), the linear geometry is favored at both the SF-CCSD and SF-CCSD(T) levels of theory, by 54.9 and 81.2 $cm^{-1}$, respectively.

While these energy differences are too small to draw any conclusions about the shape of the potential energy surface,

TABLE II. NCCCN triplet ($\tilde{X}\ ^3B_1$) state energy (in $cm^{-1}$) as a function of CCC bond angle, relative to the energy of the relaxed structure ($\angle$CCC=168.4°). (Relative state energies were calculated using B3LYP orbitals. Geometries were optimized at the UCCSD/cc-pVTZ level of theory, using HF orbitals and holding the CCC bond angle fixed.)

| | Method and basis set | | | |
|---|---|---|---|---|
| $\angle$CCC (deg) | SF-CCSD cc-pVTZ | SF-CCSD(T) cc-pVTZ | SF-CCSD aug-cc-pVTZ | SF-CCSD(T) aug-cc-pVTZ |
| 155 | 0.2 | 113.2 | | |
| 160 | −16.2 | 46.1 | | |
| 165 | −2.0 | 11.0 | | |
| 170 | 3.7 | 0.9 | | |
| 175 | 16.9 | 7.5 | | |
| 180 | 21.9 | −6.6 | −54.9 | −81.2 |

TABLE III. Relative adiabatic state energies (in eV) obtained with the NCCCN geometries shown in Table I, unless noted.

| | Method and basis set | | | |
|---|---|---|---|---|
| NCCCN state | SF-CCSD cc-pVTZ | SF-CCSD(T) cc-pVTZ | SF-CCSD aug-cc-pVTZ | SF-CCSD(T)[a] aug-cc-pVTZ |
| Triplet ($\tilde{X}\ ^3B_1/^3\Sigma_g^-$) | 0.0 | 0.0 | 0.0 | 0.0 |
| Closed-shell singlet ($\tilde{a}\ ^1A_1$) | 0.667 | 0.603 | 0.702 | 0.650 |
| Open-shell singlet ($\tilde{b}\ ^1\Delta_g$) | 0.945 | 0.820 | 0.876 | 0.746 |

[a]Using the linear structure for the triplet.

the results indicate that there is very little energy difference between the linear and bent geometries. Therefore, the $^3$NCCCN geometry is likely best described as quasilinear. The small energy differences over a wide range of geometries suggest that the CCC bending vibration undergoes large-amplitude motion.

### 2. State ordering and energies

The calculated relative energies of the triplet, closed-shell singlet, and open-shell singlet states of NCCCN are listed in Table III. The ground state is determined to be the triplet, as has been reported previously.[9,19] However, in contrast with the results of Nguyen and co-workers,[20] we find the lowest-energy singlet to be the closed-shell state, which is 0.1–0.3 eV (depending on the level of theory) more stable than the open-shell singlet state.

The predicted state ordering is consistent with the effects of the Renner–Teller coupling in the singlet state. As illustrated in Fig. 3, the two singlet states are degenerate at the linear geometry. The Renner–Teller interaction causes the states to split upon distortion from linearity, with one state ($^1A_1$) going lower in energy, and the other state ($^1B_1$) going up in energy.[39] A separate CASPT2 calculation carried out by Hrovat and Borden[40] also supports the conclusions obtained here. At the CASPT2(14,14)/aug-cc-pVTZ level of theory, the closed-shell singlet is found to lie adiabatically 0.69 eV higher in energy than the triplet state, whereas the energy of the open-shell singlet is found 0.74 eV above the triplet. These values are in excellent agreement with the SF-CCSD(T)/aug-cc-pVTZ results in Table III. Most importantly, these calculations confirm that the closed-shell singlet is the preferred singlet state, as expected for the Renner–Teller system.

### 3. Electron affinities

The adiabatic EA of $^3$NCCCN was calculated at the CCSD(T)/aug-cc-pVTZ and B3LYP/aug-cc-pVTZ levels of theory. The CCSD/cc-pVTZ geometry reported in Table I was used for the anion in the couple-cluster calculations, whereas the linear geometry (Table II) was used for the triplet state. Fully optimized geometries were used for the B3LYP calculations. The predicted and experimentally determined EA values for NCCCN are summarized in Table IV, where they are compared to those obtained by similar meth-

TABLE IV. Adiabatic EAs (binding energies) for $^3$HCCN, $^3$NCCCN, and $^1$NCCCN (in eV).

| | $^3$HCCN | $^3$NCCCN | $^3$NCCCN per Eq. (3) | $^1$NCCCN [a] |
|---|---|---|---|---|
| CCSD(T)/aug-cc-pVTZ[b] | 1.94 | 3.04 | 3.10 | 3.71[c]<br>3.75[d] |
| B3LYP/aug-cc-pVTZ | 2.02 | 3.10 | 3.08 | 3.68[c]<br>3.73[d] |
| RCCSD(T)/aug-cc-pVTZ | | 3.20[e] | | 3.67[e] |
| ACPF/aug-cc-pVTZ | | 3.36[f] | | |
| Experimental | $2.003 \pm 0.014$ [g] | $\leq 3.25 \pm 0.05$ [h]<br>$3.20 \pm 0.05$ [i] | | $3.72 \pm 0.02$ [h] |

[a]Adiabatic electron binding energy of NCCCN($\tilde{a}\ ^1A_1$).
[b]Using the geometries shown in Table I for NCCCN$^-$ and the linear geometry (Table III) for the triplet; HCCN geometries were calculated at the CCSD/cc-pVTZ level of theory.
[c]Obtained by combining the EA from the isodesmic calculation (previous column) with the SF-CCSD(T)/cc-pVTZ singlet-triplet splitting from Table III.
[d]Obtained by combining the EA from the isodesmic calculation (previous column) with the SF-CCSD(T)/aug-cc-pVTZ singlet-triplet splitting from Table III.
[e]Reference 19, RCCSD(T)/aug-cc-pVTZ//B3LYP/6-31+G(d).
[f]Reference 9.
[g]Reference 8.
[h]This work, obtained by inspection of the photoelectron spectra in Fig. 4.
[i]This work, determined from the Franck–Condon simulation of the 266 nm photoelectron spectrum, as shown in Fig. 5.

ods for HCCN. The EAs predicted by both CCSD(T) and B3LYP are in good agreement with the experimental measurements for both NCCCN and HCCN.[8]

The third column in Table IV shows the EA of $^3$NCCCN obtained using an isodesmic approach[41] based on the energetics of the electron transfer reaction

$$NCCCN^- + {}^3HCCN \rightarrow {}^3NCCCN + HCCN^- \quad (3)$$

and the known EA of HCCN.[8] The electron binding energy of the singlet state, shown in the last column in Table IV, was obtained by combining the EA calculated using the isodesmic approach with the singlet-triplet splitting calculated at the SF-CCSD(T)/aug-cc-pVTZ level of theory.

## IV. DISCUSSION

### A. Photoelectron spectrum assignment

Both NCCCN$^-$ and NCCCN have been previously studied experimentally and theoretically, but the singlet-triplet splitting and EA of the neutral have not been measured. Initial assignment of features A and B in the photoelectron spectrum (Fig. 4) can be made by comparison to the spectrum of HCCN$^-$, which shows a similar broad absorption at low eBE, corresponding to the triplet neutral state, and a sharp feature at higher eBE, assigned to the closed-shell singlet.[8] Substituting a CN group for the H to form NCCCN$^-$ yields a photoelectron spectrum similar to that of HCCN$^-$, but the observed features are shifted to higher binding energy. The large increase in eBE reflects the pseudohalogen nature of the CN group, and its ability to stabilize negative ions.[24,42,43] Therefore, band A in the NCCCN$^-$ spectra in Fig. 4 is assigned to the $\tilde{X}\,{}^3B_1/{}^3\Sigma_g^- \leftarrow \tilde{X}\,{}^2B_1$ photodetachment transition, while band B is attributed to $\tilde{a}\,{}^1A_1 \leftarrow \tilde{X}\,{}^2B_1$.

The quantitative comparison of the measured spectra with the theoretical predictions provides support for this assignment. NCCCN ($\tilde{X}\,{}^3B_1$ or ${}^3\Sigma_g^-$) is best described as a quasilinear molecule with a small barrier at the linear geometry. The large geometry change resulting from a transition from the anion structure to $^3$NCCCN results in a broad photoelectron band, consistent with band A in Fig. 4. The location of band A's origin is not clear. Examining the spectra in Figs. 4(a) and 4(b), we estimate that the band onset appears around eBE$=3.25\pm0.05$ eV. This is consistent with the computed EA values for NCCCN, which range from 3.04 to 3.36 eV depending on the method and basis set used (Table IV). There is no identifiable vibrational progression in either 266 or 355 nm spectrum. The fundamental frequency of the CCC bending vibration, which is the primary mode expected to be excited in the bent-to-linear transition, has been measured to be 102 cm$^{-1}$.[21] This mode is expected to be strongly anharmonic. This low-frequency vibration, along with other modes, makes it impossible to resolve any structure within band A. However, the VDE corresponding to the triplet state is readily determined as VDE$=3.53\pm0.02$ eV. This value compares favorably with the VDE$=3.47$ eV predicted for NCCCN$^-$ at the B3LYP/aug-cc-pVTZ level of theory.

In contrast with the NCCCN ground state, the optimized geometry of the closed-shell singlet, $\tilde{a}\,{}^1A_1$, is very similar to that of the anion (Table I). Therefore, the $\tilde{a}\,{}^1A_1 \leftarrow \tilde{X}\,{}^2B_1$ transition is expected to yield a limited Franck–Condon progression with an intense feature at the origin. The sharp feature at high eBE in the 266 nm spectrum in Fig. 4(a) (feature B) is consistent with such a transition. The band maximum at eBE$=3.72\pm0.02$ eV is assigned as the adiabatic detachment energy corresponding to the $\tilde{a}\,{}^1A_1$ state of NCCCN. This result compares remarkably well with the computed values summarized in the last column of Table IV.

The open-shell singlet state of NCCCN is calculated to be 0.74–0.82 eV (17–19 kcal/mol) higher in energy (adiabatically) than the triplet, which corresponds to an approximately 4.0 eV adiabatic detachment energy. Although the adiabatic transition is (barely) within the 266 nm (4.66 eV) photon energy range, it is not observed in our photoelectron spectra due to the poor Franck–Condon overlap expected for this bent-to-linear transition. The VDE for this transition is predicted to fall well outside the photon energy range of the experiment because the Renner–Teller splitting results in a rapid increase in the energy of the open-shell singlet state with CCC bending.

### B. EA and singlet-triplet splitting of NCCCN

It is difficult to determine the adiabatic EA and the singlet-triplet splitting in NCCCN experimentally because no features associated with the origin the triplet band (A) can be assigned. The best estimate of the band onset obtained by rather subjective inspection of the spectra in Fig. 4 places the EA at EA$\leq 3.25\pm0.05$ eV.

Greater confidence in the above experimental estimate is achieved by fitting the triplet band using a Franck–Condon simulation function. In our analysis, we used the anion and triplet geometries and frequencies calculated at the B3LYP/aug-cc-pVDZ level. Higher-level calculations do not necessarily yield better fits due to the approximations used in the modeling procedure. Namely, in order to avoid having to evaluate the multidimensional overlap integrals of vibrational wave functions, the simulation uses the parallel-mode approximation and assumes harmonic oscillators, as described in detail elsewhere.[42] Several important limitations of this method should be recognized. First, the NCCCN$^-$ anion is bent, while the $^3$NCCCN neutral is quasilinear. Therefore, one rotational mode of the anion becomes a vibration in the neutral. To simplify the analysis, we opted to optimize the $^3$NCCCN geometry with a CCC angle arbitrarily fixed at 175° to allow overlap of all vibrational modes. Second, band A has no resolved vibrational progression with which to compare simulated progressions. Third, the use of the parallel-mode approximation may be questioned in this case, as it is most appropriate for small geometry changes, which is hardly the case in $^3$NCCCN$\leftarrow$NCCCN$^-$ photodetachment. Finally, the potential energy surface for CCC bending is highly anharmonic, so evaluating overlap integrals of these principal Franck–Condon active modes requires additional computational effort.

In fitting the triplet band, we matched band A maximum and shape in the 266 nm spectrum by scaling vibrational energies and convoluting all peaks with Gaussian functions

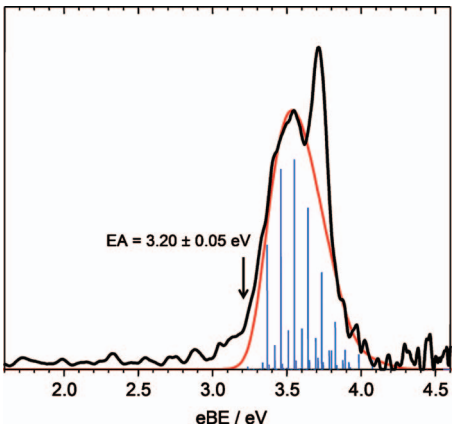


FIG. 5. Simulation of photoelectron band A using a Franck–Condon fitting procedure and geometries and frequencies obtained from B3LYP/aug-cc-pVDZ calculations. The black solid line is the experimental spectrum reproduced from Fig. 4(a). The red line is the convoluted fit from the simulation. The blue vertical lines are the calculated Franck–Condon factors. The arrow indicates the adiabatic EA obtained by fitting the Franck–Condon simulation to the experimental spectrum.

of variable width.[44] Although this procedure is admittedly crude, it produces a satisfactory fit; an example is shown in Fig. 5. The parameters used to model the 266 nm spectrum also produce a satisfactory fit of the onset of band A in the 355 nm spectrum, after accounting for differences in resolution. Our simulation for band B confirms that this feature is a vertical transition to the ground vibrational state of $^1$NCCCN.

The predicted intensity at the origin is negligible, as one expects for a weak transition resulting from a large change in geometry. Still, this fitting procedure yields an adiabatic EA of $EA=3.20\pm0.05$ eV, which is an improvement compared to the upper-limit estimate ($EA\leq3.25\pm0.05$ eV) obtained by simply inspecting the spectra (see Table IV). Using this value in conjunction with the origin of the singlet band at $3.72\pm0.02$ eV, we estimate the singlet-triplet ($\tilde{a}\,^1A_1\leftarrow\tilde{X}\,^3B_1/^3\Sigma_g^-$) splitting in NCCCN as $\Delta E_{ST}=0.52\pm0.05$ eV ($12.0\pm1.2$ kcal/mol). This estimate compares well with the theoretical value of 13.9 kcal/mol obtained with SF-CCSD(T)/cc-pVTZ, the highest level of theory employed in this study.

## V. CONCLUSIONS

The photoelectron imaging study of $NCCCN^-$ reveals two bands in the photoelectron spectrum, corresponding to a triplet ground state ($\tilde{X}\,^3B_1$ or $^3\Sigma_g^-$) and an excited closed-shell singlet state ($\tilde{a}\,^1A_1$). Theoretical calculations show that the triplet is either quasilinear or linear. The triplet potential energy surface for CCC bending is flat and therefore sensitive to the choice of theoretical method and basis set. In contrast, the closed-shell singlet has a geometry very similar to the anion. Correspondingly, the singlet state is characterized by a sharp feature in the photoelectron spectrum, whereas the triplet state is represented by a broad, congested band. The best estimate of the origin of the triplet band, supported by the Franck–Condon modeling, yields an adiabatic EA of NCCCN, $EA=3.20\pm0.05$ eV. The adiabatic electron binding energy of the closed-shell singled state is measured to be $3.72\pm0.02$ eV, while the singlet-triplet ($\tilde{a}\,^1A_1\leftarrow\tilde{X}\,^3B_1/^3\Sigma_g^-$) splitting is determined as $\Delta E_{ST}=0.52\pm0.05$ eV ($12.0\pm1.2$ kcal/mol).

The second CN group on NCCCN does not significantly alter the singlet-triplet gap, compared to cyanocarbene [$\Delta E_{ST}(HCCN)=0.516$ eV].[8] For comparison, the difference in singlet-triplet splittings of HCH and HCCN is about 0.39 eV,[2,8] a clear example of resonance stabilization. Our work illustrates an important point, however, that $\Delta E_{ST}$ is the magnitude of the singlet-triplet gap—and is only indirectly related to resonance stabilization of unpaired electrons in one of the states. Thus, a possible explanation for the similar $\Delta E_{ST}$ of NCCCN and HCCN is that while the triplet ground state of NCCCN might have increased resonance stabilization, the Renner–Teller splitting on the singlet surface drives the singlet state energy down as well, so the relative energy gap between the singlet and triplet states remains approximately unchanged.

## ACKNOWLEDGMENTS

This work was supported by the U.S. National Science Foundation under Grant No. CHE-0713880 (A.S.) and Grant Nos. CHE-0454874 and CHE-0808964 (P.W.). Calculations were carried out using the resources from the Center for Computational Studies of Open-Shell and Electronically Excited Species (http://iopenshell.usc.edu), directed by Professor Anna Krylov. We thank Professor Lyudmila Slipchenko for assistance with the electronic structure calculations and Dr. David Hrovat and Professor Weston T. Borden for providing the results of their CASPT2 calculations.

[1] P. C. Engelking, R. R. Corderman, J. J. Wendoloski, G. B. Ellison S. V. ONeil, and W. C. Lineberger, J. Chem. Phys. **74**, 5460 (1981).
[2] D. G. Leopold, K. K. Murray, A. E. S. Miller, and W. C. Lineberger, J. Chem. Phys. **83**, 4849 (1985).
[3] A. Rauk, *Orbital Interaction Theory of Organic Chemistry* (Wiley, New York, 1994).
[4] R. L. Schwartz, G. E. Davico, T. M. Ramond, and W. C. Lineberger, J. Phys. Chem. A **103**, 8213 (1999).
[5] H. Tomioka, Acc. Chem. Res. **30**, 315 (1997).
[6] N. P. Bowling, R. J. Halter, J. A. Hodges, R. A. Seburg, P. S. Thomas, C. S. Simmons, J. F. Stanton, and R. J. McMahon, J. Am. Chem. Soc. **128**, 3291 (2006).
[7] P. S. Thomas, N. P. Bowling, and R. J. McMahon, J. Am. Chem. Soc. **131**, 8649 (2009).
[8] M. R. Nimlos, G. Davico, C. M. Geise, P. G. Wenthold, W. C. Lineberger, S. J. Blanksby, C. M. Hadad, G. A. Petersson, and G. B. Ellison, J. Chem. Phys. **117**, 4323 (2002).
[9] J. Kalcher, Chem. Phys. Lett. **403**, 146 (2005).
[10] C. L. Morter, S. K. Farhat, and R. F. Curl, Chem. Phys. Lett. **207**, 153 (1993).
[11] R. A. Bernheim, R. J. Kempf, and E. F. Reichenbecher, J. Magn. Reson. (1969-1992) **3**, 5 (1970).
[12] R. A. Bernheim, R. J. Kempf, J. V. Gramas, and P. S. Skell, J. Chem. Phys. **43**, 196 (1965).
[13] R. A. Bernheim, R. J. Kempf, P. W. Humer, and P. S. Skell, J. Chem. Phys. **41**, 1156 (1964).
[14] E. Wasserman, W. A. Yager, and V. J. Kuck, Chem. Phys. Lett. **7**, 409 (1970).
[15] K. S. Kim, H. F. Schaefer III, L. Radom, J. A. Pople, and J. S. Binkley, J. Am. Chem. Soc. **105**, 4148 (1983).
[16] J. C. Poutsma, S. D. Upshaw, R. R. Squires, and P. G. Wenthold, J. Phys. Chem. A **106**, 1067 (2002).
[17] E. Wasserman, L. Barash, and W. A. Yager, J. Am. Chem. Soc. **87**, 2075

(1965).
[18] I. R. Dunkin and A. McCluskey, Spectrochim. Acta, Part A **50**, 209 (1994).
[19] S. J. Blanksby, S. Dua, J. H. Bowie, D. Schroeder, and H. Schwarz, J. Phys. Chem. A **104**, 11248 (2000).
[20] B. Hajgato, R. Flamming, T. Veszpremi, and M. T. Nguyen, Mol. Phys. **100**, 1693 (2002).
[21] G. Maier, H. P. Reisenauer, and R. Ruppel, Eur. J. Org. Chem. **2003**, 2695 (2003).
[22] R. R. Lucchese and H. F. Schaefer, J. Am. Chem. Soc. **99**, 13 (1977).
[23] L. Velarde, T. Habteyes, and A. Sanov, J. Chem. Phys. **125**, 114303 (2006).
[24] D. J. Goebbert, L. Velarde, D. Khuseynov, and A. Sanov, J. Phys. Chem. Lett. **1**, 792 (2010).
[25] A. Eppink and D. H. Parker, Rev. Sci. Instrum. **68**, 3477 (1997).
[26] D. W. Chandler and P. L. Houston, J. Chem. Phys. **87**, 1445 (1987).
[27] A. J. R. Heck and D. W. Chandler, Annu. Rev. Phys. Chem. **46**, 335 (1995).
[28] V. Dribinski, A. Ossadtchi, V. A. Mandelshtam, and H. Reisler, Rev. Sci. Instrum. **73**, 2634 (2002).
[29] C. Valli, C. Blondel, and C. Delsart, Phys. Rev. A **59**, 3809 (1999).
[30] D. M. Neumark, K. R. Lykke, T. Andersen, and W. C. Lineberger, Phys. Rev. A **32**, 1890 (1985).
[31] J. Cooper and R. N. Zare, J. Chem. Phys. **48**, 942 (1968).
[32] J. Cooper and R. N. Zare, J. Chem. Phys. **49**, 4252 (1968).
[33] S. V. Levchenko and A. I. Krylov, J. Chem. Phys. **120**, 175 (2004).
[34] A. I. Krylov, Chem. Phys. Lett. **350**, 522 (2001).
[35] L. V. Slipchenko and A. I. Krylov, J. Chem. Phys. **123**, 084107 (2005).
[36] S. V. Levchenko, H. Reisler, A. I. Krylov, O. Gessner, A. Stolow, H. C. Shi, and A. L. L. East, J. Chem. Phys. **125**, 084301 (2006).
[37] L. V. Slipchenko and A. I. Krylov, J. Chem. Phys. **117**, 4694 (2002).
[38] Y. Shao, L. F. Molnar, Y. Jung, J. Kussmann, C. Ochsenfeld, S. T. Brown, A. T. B. Gilbert, L. V. Slipchenko, S. V. Levchenko, D. P. O'Neill, R. A. DiStasio, Jr., R. C. Lochan, T. Wang, G. J. O. Beran, N. A. Besley, J. M. Herbert, C. Y. Lin, T. Van Voorhis, S. H. Chien, A. Sodt, R. P. Steele, V. A. Rassolov, P. E. Maslen, P. P. Korambath, R. D. Adamson, B. Austin, J. Baker, E. F. C. Byrd, H. Dachsel, R. J. Doerksen, A. Dreuw, B. D. Dunietz, A. D. Dutoi, T. R. Furlani, S. R. Gwaltney, A. Heyden, S. Hirata, C.-P. Hsu, G. Kedziora, R. Z. Khalliulin, P. Klunzinger, A. M. Lee, M. S. Lee, W. Liang, I. Lotan, N. Nair, B. Peters, E. I. Proynov, P. A. Pieniazek, Y. M. Rhee, J. Ritchie, E. Rosta, C. D. Sherrill, A. C. Simmonett, J. E. Subotnik, H. L. Woodcock III, W. Zhang, A. T. Bell, and A. K. Chakraborty, Phys. Chem. Chem. Phys. **8**, 3172 (2006).
[39] Although the open-shell singlet in NCCCN is calculated to be linear, the state can be bent in other systems, including methylene, CH2.
[40] D. A. Hrovat and W. T. Borden, private communication (2009).
[41] N. R. Wijeratne, M. Da Fonte, A. Ronemus, P. J. Wyss, D. Tahmassebi, and P. G. Wenthold, J. Phys. Chem. A **113**, 9467 (2009).
[42] D. J. Goebbert, D. Khuseynov, and A. Sanov, J. Phys. Chem. A **114**, 2259 (2010).
[43] D. J. Goebbert, D. Khuseynov, and A. Sanov, J. Chem. Phys. **131**, 161102 (2009).
[44] H. J. Deyerl, L. S. Alconcel, and R. E. Continetti, J. Phys. Chem. A **105**, 552 (2001).